Analysis of dynamic properties of the PRT vehicle-track system

M. KOZŁOWSKI, W. CHOROMAŃSKI*, and J. KOWARA

Faculty of Transport, Warsaw University of Technology, 75 Koszykowa St., 00-662 Warszawa, Poland

Abstract. The paper presents the issue of modelling the system of the PRT vehicle – track. The PRT – Personal Rapid Transit concept is defined as an innovative transport system composed of small vehicles (3–5 persons) moving on the light infrastructure situated at a height of above 5 meters above the ground. This is a system that combines the features of individual and public transport. An important feature of this system is the implementation of the transport approach known as the 'point to point' rule that is to say between the initial and the final stop the vehicle does not stop at the intermediate stops. The vehicle has no driver. Routing choice and collision avoidance are performed through a complex computer system.

Key words: APM, ATS, Personal Rapid Transit, PRT, modeling, scale model, MBS.

1. Introduction

The subject of the article is the dynamics of a PRT vehicle. As indicated in the abstract, the PRT [1, 2] concept is the new transport system which belongs to the class of APM & ATS systems (Automated People Movers and Automated Transit System) [3, 4]. Recently PRT vehicles and systems have been identified with the term PodCar [5]. It should be noted that such systems may be undertaken in very different ways in terms of design solutions. Work on the construction of this system has also been launched at the Warsaw University of Technology. This work is being undertaken within the Eco-Mobility project financed by the Innovative Economy Operational Programme. This paper focuses on the analysis of the dynamic behaviour which is examined in several stages (iteratively):

1. On the basis of the designers' idea, a construction of a full-scale model and analysis by performing computer simulations.
2. Determining the parameters of the system in a scale and the construction of physical model in a scale. The simulation testing of a scale model and testing of a physical scale model.
3. On the basis of the conclusions from performing the points 1 and 2, the simulation testing of a full-scale model (preceded by verification tests and after performing the point 4 proceeded by validation of simulation model).
4. The construction of the physical model in a full scale and experimental studies.

In general, the points 1–4 are carried out iteratively. Some of the concepts used in this paper should be explained. What is called a generic model is an idealized model which results from the analysis of the physical model or of a concept of this model. This idealized model consists of discrete masses (including their distribution) and reacting elements, etc. The important decisions regarding the nature of this model are made at this stage already. In this work an arbitrary

decision has been taken, that the model deals with lumped parameters, determined and continuous in time. Based on the generic model, a mathematical model is being built and then a simulation model (which is a representation of the model in a specific programming environment, such as C, Matlab, etc.). In this case, the operations are done automatically using MBS (MultiBody Systems) packages, more specifically using SIMMechanics software running in the environment of Matlab ver 13. Additionally, for analysis of the contact forces between the polyurethane wheels of the PRT vehicle and the track, the package DefTire has been used (his strategy was also used in the vehicle dynamics studies [6,7]). Such a strategy for analysis of the dynamic properties of the vehicle is dictated by the important substantive and economic considerations:

a) The construction of the experimental track to a scale 1:1 is very expensive, however at the stage of vehicle certification it is required. The construction of a scale 1:4 would be certainly less expensive.
b) Tests to scale, if carried out properly, allow to draw conclusions about the full scale design.
c) In the simulation tests targeted at the implementation, the ability to make rapid changes not only for the design parameters but also for the design structure itself, is of fundamental importance - hence the use of MBS packages.

Achieving all of the aforementioned points is a very complex and time consuming process. In the current stage of the project, a full scale vehicle model has been constructed. The construction of an experimental track (which is the most expensive) has yet to be done. This paper focuses on the problems contained in point 2, more precisely on the problems related to the construction and testing of a scale 1:4 simulation model (the geometric scale). As already mentioned, it is an important element in the test programme on the dynamics of the PRT vehicle. The results of simulation studies on parametric sensitivity of the model of the real dimensions 1:1 presented in [11].

---

*e-mail: prof.wch@gmail.com

1.1. Physical object. Scale model. Carrying out point 1 has led to the carrying out the process of scaling and constructing a scale physical model shown in Fig. 1.
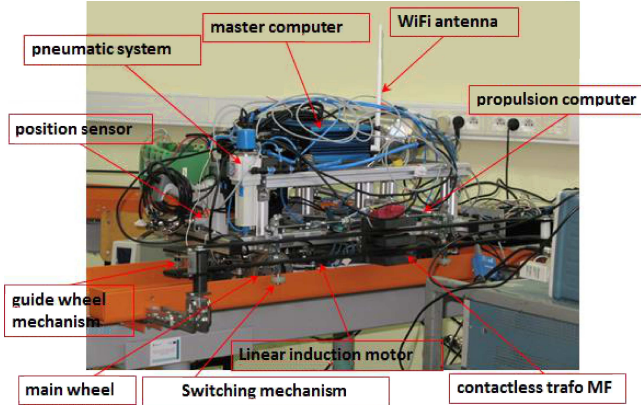

Fig. 1. Physical PRT model in 1:4 scale

The similarity scales result from the principles of similarity which are fully described in the literature, concerning for example the scale tests of ocean – going vessels. In comparison with mechanical objects such as the rail vehicle, the method used is described in details in [8]. In relation to the PRT vehicle analysed, the authors present this method in detail in [9]. This is just summarised as follows:

An initial point for defining the relation of similarity is determining a length scale coefficient and the general conditions. These conditions are listed below, where k_l is determined as the scale coefficient for the l length and k_t as the scale coefficient for t time, wherein the full-size length is determined with index "1" and the length of scale model – with index "0".

$$k_l = l_1/l_0, \qquad k_t = t_1/t_0. \tag{1}$$

Using the above coefficients, a scale coefficient has been determined for the k_A cross-section, k_V volume, k_v velocity and k_a acceleration.

$$k_A = k_l^2, \quad k_V = k_l^3, \quad k_v = k_l/k_t, \quad k_a = k_l/k_t^2. \tag{2}$$

For the density ρ, the scale coefficient is respectively:

$$k_\rho = \rho_1/\rho_0. \tag{3}$$

Then the scale coefficients for k_m mass, k_I moment of inertia, k_F inertia forces, respectively:

$$k_m = k_\rho * k_l^3, \qquad k_I = k_m * k_l^2,$$
$$k_F = \frac{m_1 * a_1}{m_0 * a_0} = k_m * k_a = \frac{k_\rho k_l^4}{k_t^2} \tag{4}$$

and for the frequency the result is:

$$k_f = 1/k_t. \tag{5}$$

The purpose of constructing the model is to replicate dynamic behaviour in the vehicle movement on a linear and a curved track, in the range of acceleration, whilst passing through the junction and in a braking operation.

In general, the basic equation of motion is expressed as a balance of forces acting on the system, for a similarity, a scale coefficient k_F should be determined for all the forces included in Eq. (6).

$$m\ddot{x} + c\dot{x} + kx = F \tag{6}$$

in a polar coordinate system the equation (7) is obtained corresponding to

$$I\ddot{\theta} + c_T\dot{\theta} + k_T\theta = T, \tag{7}$$

where m – weight, I – moment of inertia, c, c_T – damping coefficients, k, k_T – coefficients of elasticity, F – forces acting, T – torque applied.

Correspondingly, for the scale model this gives:

$$m\ddot{x}\left(\frac{k_m k_l}{k_t^2}\right) + c\dot{x}\left(\frac{k_c k_l}{k_t}\right) + kx\,(k_k k_l) = F(k_F), \tag{8}$$

$$\left(\frac{k_m k_l}{k_t^2}\right) = \left(\frac{k_c k_l}{k_t}\right) = (k_k k_l) = (k_F). \tag{9}$$

Using the above defined scale coefficients the dependencies (10) and (11) are obtained, the results of which provide the comparisons for the scale model.

$$k_l^4 = k_c k_l = k_k k_l = k_F, \tag{10}$$

$$k_c = k_l^3, \qquad k_k = k_l^3, \qquad k_F = k_l^4. \tag{11}$$

To obtain a full similarity, it is necessary to obtain the scaling coefficients for the forces, acting in the contact between wheels and the track, Describing and defining these forces requiring the knowledge of the equations describing an impact on the selected type of contact.

As can be seen, due to the constructional limitations including the linear motor assembly [ ] the coefficients shown in Table 1 allow only a partial similarity to be achieved.

Table 1
Finally, there are used the following scale coefficients

Lp.	Applies to dimension:	The values of scale coefficients	Symbol
1	length	4	k_l
2	time	2	k_t
3	density	1/2	k_ρ
4	frequency	1/2	k_f
5	surface	16	k_A
6	volume	64	k_V
7	weight	32	k_m
8	velocity	2	k_v
9	acceleration	1	k_a
10	inertia forces	32	k_F
11	moments of inertia	512	k_I

Figure 1 shows the physical scale model. Certain elements not seen in the picture should be commented on. Polyurethane wheels, on which the vehicle is mounted, operate in a wheel set with independently turning wheels.

2. Generic Scale model of PRT vehicle in scale. The geometry for running gear system of PRT vehicle model

Figure 2 shows a 1:4 scale model of the PRT vehicle [10]. The origin point of coordinate system has been placed at the rectangular projection point of the centre of gravity on the plane of the road surface. Indicated: B – mass of the vehicle body suspended elastically (blue), a_1 – front steer axle (red), a_2 – rear steer axle (red), a_{LP1}, a_{LP2} – steering arms of external rollers (green), LP1, LP2 – internal rollers of left-front quarter of the vehicle (black), LPZ – external roller of the left front quarter of the vehicle (black), W_{LP} – tired wheel of the left front quarter of the vehicle (remaining rollers and wheels marked with indexes indicating the quarters of the vehicle). The modelling scheme of the external rollers is structurally asymmetrical. For safety reasons, the model lowers only one system of right or left rollers. A model with lowered left system of external rollers (shown in Fig. 2) is designed for the analysis of motion on the left-curving tracks. The basic geometrical dimensions are shown in Table 2.
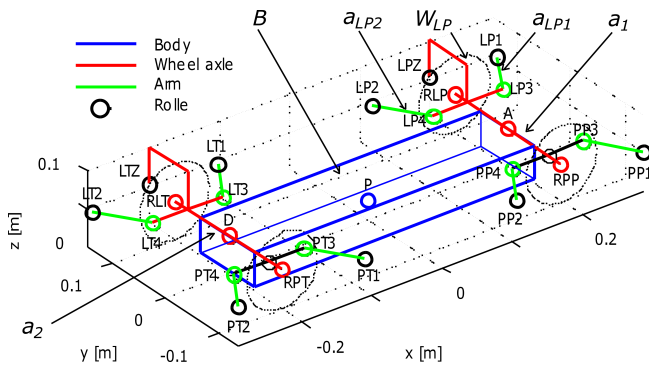

Fig. 2. Generic model of PRT vehicle in 1:4 scale

Table 2
The basic geometric data (roller supports coordinates for the left front quarter – the vehicle is symmetrical relative to the axis OX and OY)

Symbol	Description	Value [m]
L	a distance between axles of vehicle wheels	0.4
D	a vehicle wheelbase	0.2
r	a dynamic tyre radius	0.05
P	the centre of gravity	[0 0 0.0275]
A	The centre of the front	[0.2 0 0.05]
D	the centre of the rear	[−0.2 0 0.05]
$LP1$	Roller 1 left front	[0.29 0.136 0.05]
$LP2$	Roller 2 left front	[0.11 0.136 0.05]
LPZ	External roller left front	[0.2 0.146 0.05]
$LP3$	Support 3 left front	[0.25 0.075 0.05]
$LP4$	Support 4 left front	[0.15 0.075 0.05]
RLP	The wheel centre left front	[0.2 0.1 0.05]

3. Kinematical analysis of bend curvature of the guide rail

The aim of kinematic calculations is to examine the properties of geometric paths of movement of the vehicle rollers,

which is treated as a rigid body. It is assumed, that the centre point of mass of vehicle moves along the set curve, and the steering axles of vehicle are setting radially along the bend radius. To describe the return curve, a segment of the circular arc is used or a Track Transition Curve (biclothoid).

Figure 3 shows the geometric assumptions for the analysis of kinematic paths of movements for the vehicle at selected points for cornering. The curve marked "1" is a fragment of a circular arc connecting the O start point with the Z end point of the turn. To draw the arc it has been assumed $OX = 2$ m, angle of return $\alpha_Z = 45°$. A radius of the circular arc $R = 2.82$ m. Fulfilling the condition of radial positioning the vehicle with a length $l = 0.4$ m in this arc requires a symmetric turn of both vehicle axles with a steering angle $\alpha_a = 4.05°$. Curve "2" is a Track Transition Curve (biclothoid). A twist of vehicle axles takes place on the longest road section (the velocity of axles twisting is the smallest). The K point is where symmetric clothoids are stuck together. At this point the steering angle of the vehicle axle (in conditions of radial setting in a bend) reaches the maximum value $2\alpha_a = 8.10°$. (In the calculations there have been used generally known dependencies).
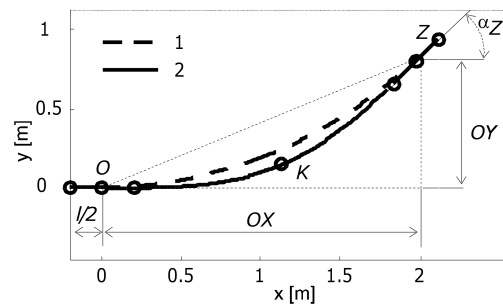

Fig. 3. Trajectories of movement of the point of vehicle centre: 1 – circular arc, 2 – Track Transition Curve (biclothoid) of a constant turning velocity of the vehicle both axles

Figure 4 shows fragments of trajectories of the selected rollers (of the vehicle treated as a rigid body) travelling on the Track Transition Curve (biclothoid) (chart "3" Fig. 3). A turn to the left requires a constant contact of the left front internal
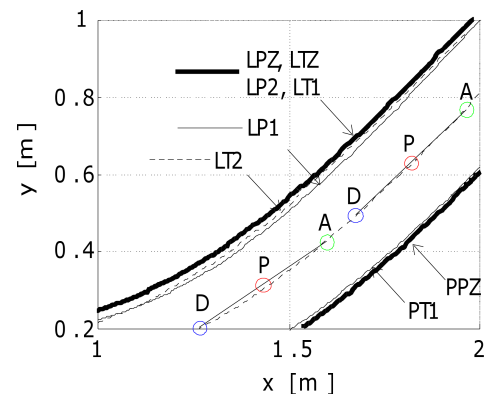

Fig. 4. Segments of trajectories of the vehicle selected rollers (the centre of gravity P moves along the Track Transition Curve (biclothoid) – curve "2" Fig. 3)

roller with the rail edge. For this reason it has been assumed that the track edge is a specified LPZ curve (Fig. 4). The results show that the placement of rollers (Table 2) is correct as none of the shown trajectories intersect with the LPZ curve describing the assumed edge of the rail. There are no geometric obstacles for the radial setting of vehicle in a bend, where this may contribute to a symmetric working together of rollers with the rail edge and to the correct dynamics of the motion in a bend.

4. Dynamic model of a PRT vehicle

The purpose of developing a dynamic model is a description of the vehicle motion based on the knowledge of forces acting on it. The 1:4 generic scale model of a PRT vehicle is shown in Fig. 2. Figure 5 shows the generic model of the body panel suspension on the vehicle axle. Marked: a – the axle of wheels (parallel to OX axis of the vehicle reference system Fig. 2), d – longitudinal axis of the vehicle body (parallel to OY axis of the vehicle reference system Fig. 2), A – suspension point of the body chassis on the axle of wheels. It has been assumed that the axle of the wheels has a movement with 3 degrees of freedom relative to the body chassis: revolute 1 – a rotation relative to the d axis (deviation *roll//roll* deviation), revolute 2 – a rotation relative to the h axis (deviation *yaw*) and prismatic 1 – a linear displacement along the h axis. The range of movement is limited by elastic forces and damping of the model. Marked: c_{r1}, c_{r2}, k_{r1}, k_{r2} – torsional elasticity and damping, c_{p1}, k_{p1} – linear elasticity and damping. Figure 6 shows the generic model of a guide roller for the PRT vehicle. The model consists of the following elements: 1 – a point of the roller, 2 – a point of the rail marker (a potential point of a roller contact with a rail), 3 – a point moving along a setpoint curve, 4 – a guide rail, 5 – limiting degrees of freedom for the movement of the roller point relative to the rail marker, limiting to the condition of movement on the ZOX plane of the vehicle chassis as a local reference system, 6 – a roller arm, 7 – an elastic and damping element with nonlinear characteristics, c_{pr}, k_{pr} – nonlinear elasticity and damping, d_r – a distance of the roller point relative to the tangent to the rail edge, l – a curve of the roller edge, λ – a tangent to the rail
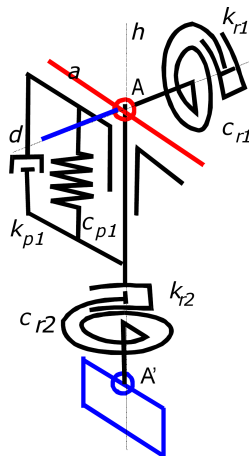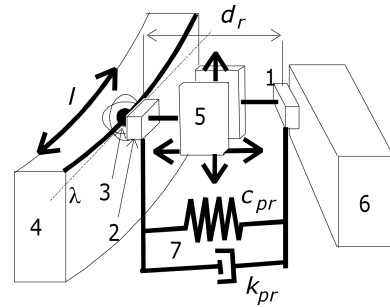
edge in a potential contact point. The model generates the contact forces if the roller material point passes to a negative half-plane defined by the tangent line λ. A modelled contact force has two components: normal and tangential. Figure 7

Fig. 6. Roller model
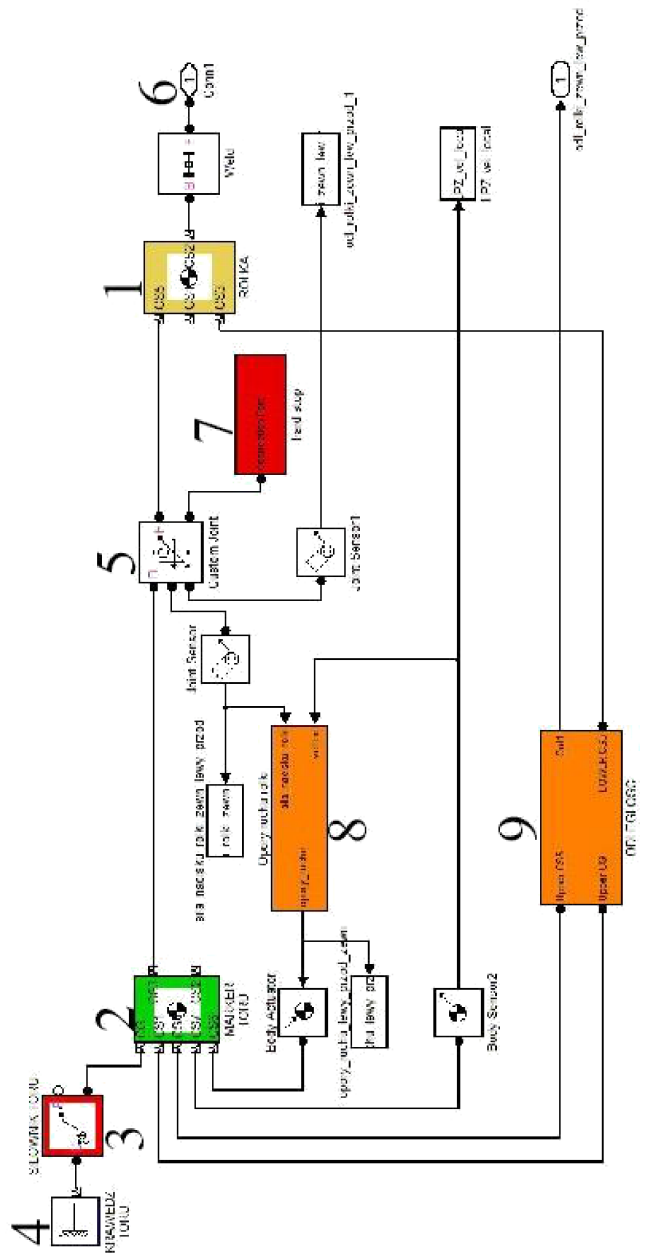

Fig. 5. Suspension model

Fig. 7. Structure of calculation model of roller contact forces

shows only the actuator 7 used to generate a normal force. A tangential force, modelling resistance forces of rolling a roller at the moment of contact, is applied to the block of roller 1 in direction of λ tangent (in such a way that a force sense is opposite to the direction of motion).

The structure of a simulation model of the roller system is shown in Fig. 7. The symbols of elements are the same as in Fig. 6. Additional calculation blocks are marked: 8 – a calculation block for the rolling resistance of roller bearings at the moment of contact, 9 – a control block defining a roller-rail distance relative to a tangent of motion curvature in a point of contact.

Operating principle of the roller calculation block is illustrated in Fig. 8: a) distances of rollers, relative to the tangent to the rail edge curvature at the point of a potential contact, b) contact force of rollers on the rail edge. The charts are marked: "1" – LP1 roller, "2" – LP2 roller, "3" – LPZ roller. A radial contact force (representing the force of the roller on the rail is created under the elastic-damping impact causing a minimal deformation of the rail edge – symbols t_1, t_2 and t_3 indicate moments when of the individual rollers are in contact with a rail edge. In moments of contact there are also calculated tangential forces (not shown in the picture), modelling the rolling resistances of roller bearings.
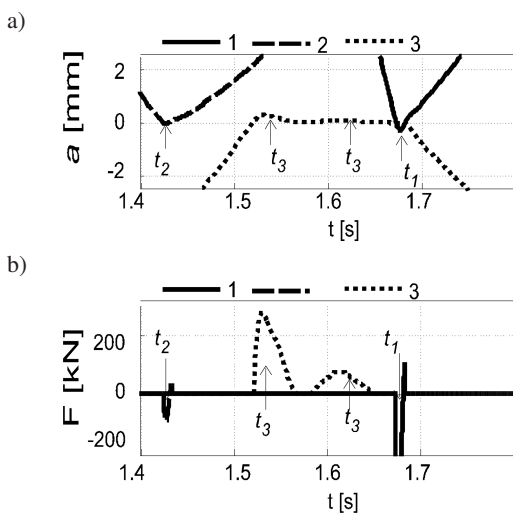

Fig. 8. Instantaneous simulation waveforms illustrating the rollers operation: a) a distance of rollers against the tangent to the curvature of the rail edge at the point of potential contact, b) a contact force of rollers on the rail edge

5. Model parameters

Dynamic parameters are adopted on the basis of the design made in Catia. The basic geometrical dimensions are shown in Table 2. In addition, it has been assumed that the vehicle weight is $m_P = 20$ kg, and the torques relative to the fundamental rotation axes are equal to: $J_{xx} = 1$ kgm^2, $J_{yy} = 1$ kgm^2, $J_{zz} = 1$ kgm^2. The values of elastic – damping elements are put together in Table 3. The MBS simulation model has been made in SimMechanics programme. A library simulation model of wheel and tyre developed

by TNO. The tyre parameters are described with a file 'TNO_express_tyre_PRT.tir', enabling an individual selection of values. For a tyre with a radius $R_0 = 0.05$ m and a width $d_0 = 0.02$ m, the following values are applied for elasticity and damping in the vertical direction $c_v = 1850000$ N/m, $k_v = 5000$ Ns/m.

Table 3
Basic elastic-damping elements

Symbol	Value
c_{r1}	300 N/rad
c_{r2}	15 N/rad
k_{r1}	20 Ns/rad
k_{r2}	1 Ns/rad
c_{pr}	40 kN/m
k_{pr}	3.5 kNs/m

6. Conditions of calculating

For the cornering conditions – external rollers take over driving a vehicle. A motion curvature profile determines the inertia forces accumulation, acting as a primary reason of contact. A corner profile can be described using curve nodes of the roller edges. In the model presented there are divided two basic types of curves: circular arc or biclothoid (Fig. 3). The physical model of vehicle never has right and left external rollers lowered at the same time. The system of external rollers is structurally asymmetrical for selected turning directions (turning left or right). Therefore, the models can be defined for example left- or right-rotating. Further asymmetry of the model gear-system may relate to for example limitation of steering freedom of vehicle wheel axles. Consideration of these limitation may lead to identifying the following specific models of a vehicle: a model with a rigid axles of wheels, a model with rear rigid axle and front steering axle, a model with both steering axles. Additional differences in modelling may concern the assumed initial conditions of movement. In relation to the track axis, the initial position of the vehicle body can be co-axial, torsional or shifted.

7. The simulation results

For carrying out simulation tests, it is assumed that the required trajectory is composed of three parts: a straight section of 2 m length entry, a bend with 45° return angle on the longitudinal section $OX = 2$ m (for which the curvature graph is shown in Fig. 3) and a straight section of 2 m length exit. It is assumed that the vehicle moves with a constant velocity $v = 1$ m/s. The required curvatures of rail edges and track centre resulting from earlier studies of kinematics (the results of which are shown in Fig. 4). Figure 9 shows a schematic diagram of the position of the simulation model blocks at the time $t_s = 3.4$ s. Marked: P – a geometric centre point of chassis block (corresponding to the vehicle gravity centre), A – a centre point of the front steering axle a_1, D – a centre point of the rear steering axle, λ_1 – a curve representing an edge of the left rail, λ_2 – a curve representing an edge of the right rail, λ_0 – a curve representing a hypothetical centre

of the track, n_1 – a perpendicular line to the curvature of track axis centre passing through the A point – a centre of the front steering axle, n_2 – a perpendicular to the curvature of the track axis centre passing through the D point centre of the rear steering axle, n_0 – a perpendicular to the curvature of the track axis centre passing through the P point a geometric centre of the vehicle chassis body, ψ_A – a turn angle of n_0 perpendicular. The markings enable the specifying of the state variables describing the position of vehicle blocks just like it is done in the description of the rail vehicle dynamics, namely: y_1 – a distance of the point A of the front axle centre from the λ_0 track centre, ψ_1 – a front axle deviation angle a_1 from the n_1 perpendicular, y_2 – a distance of the point D of the rear axle centre from the λ_0 track centre, ψ_2 – a rear axle deviation angle a_2 from the n_2 perpendicular, y_0 – a distance of the P point – a geometric centre of the vehicle chassis body from the λ_0 track centre, ψ_0 – a deviation angle of the chassis block axis from the required motion direction. The values of A, D and P point coordinates for the simulation moment are presented in the description of Fig. 9.
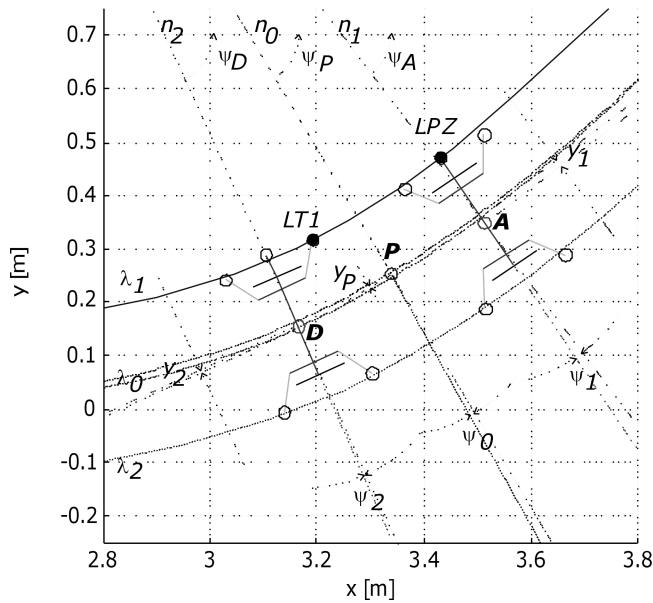
Fig. 9. Schematic diagram of the simulation model position at the time $t_s = 3.4$ s. The values of the state variables are $P(x = 3.339,$ $y = 0.253)$ m, $P(\lambda_0 = 3.386, y_P = -0.0016)$ m, $A(x = 3.513,$ $y = 0.351)$ m, $A(\lambda_0 = 3.585, y_1 = -0.0068)$, $D(x = 3.164,$ $y = 0.155)$ m, $D(\lambda_0 = 3.1855, y_2 = 0.0036)$ m, $\psi_P = -59.1735°,$ $\psi_A = -52.962°,$ $\psi_D = -65.428°,$ $\psi_0 = -1.488°,$ $\psi_1 = -3.121°,$ $\psi_2 = 0.3265°$.

In the position shown in Fig. 9 a vehicle is deviated from the ideal trajectory. For this reason, LPZ and LT1 rollers are in contact with a rail edge. Instantaneous waveforms of the state simulation variables are illustrated by the graphs shown in Figs. 10, 11 and 12.

Graph 10 represents the setting of vehicle axle relative to the track centre: a) the lateral deviations, b) steering angles relative to the perpendicular line.

Graph 11 represents instantaneous waveforms of forces in the roller systems: a) font, b) rear.

Graph 12 represents waveforms of slip angles (sideslip angle alpha) of the vehicle wheel tyres: a) front, b) rear.
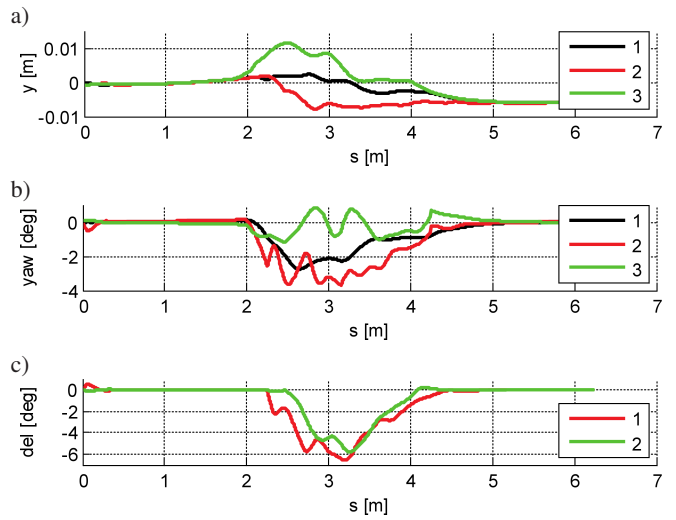
Fig. 10. Charts of vehicle axle settings relative to the track centre: a) lateral deviations, b) turning angles relative to the perpendicular line. The charts are marked: $1 - y_0$, $2 - y_1$, $3 - y_2$, $1 - \psi_0$, $2 - \psi_1$, $3 - \psi_2$
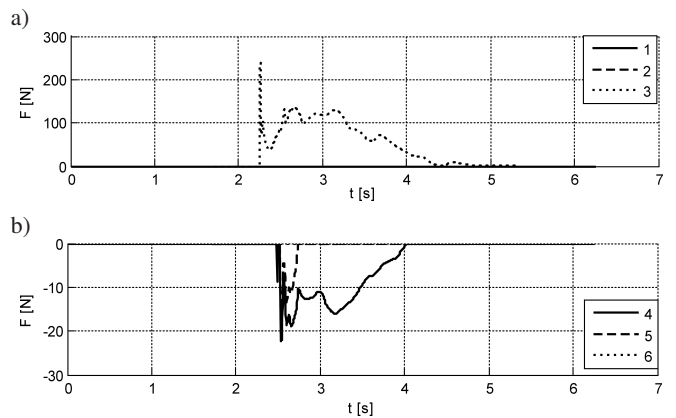
Fig. 11. Instantaneous waveforms of forces in the systems of rollers: a) front, b) rear. The charts are marked: 1 – LP1, 2 – LP2, 3 – LPZ, 4 – LT1, 5 – LT2, 6 – LTZ
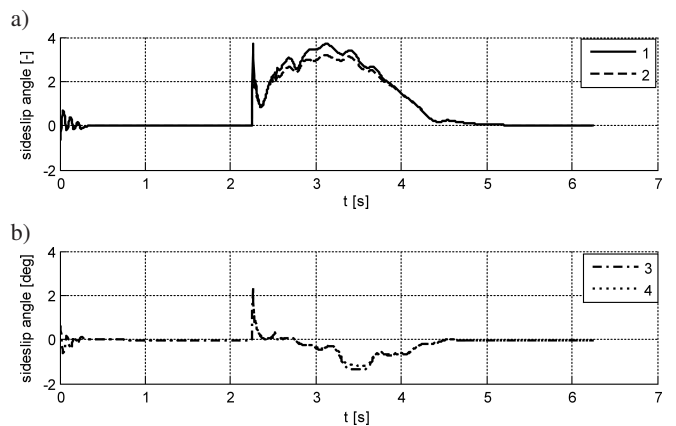
Fig. 12. Waveforms of slip angles (sideslip angle alpha) of the vehicle wheels tyres: a) front, b) rear. The charts are marked: 1 – left front, 2 – right front, 3 – left rear, 4 – right rear

Figure 13 shows the waveforms of longitudinal slip (longitudinal slip) of the vehicle wheel tyres: a) front, b) rear.
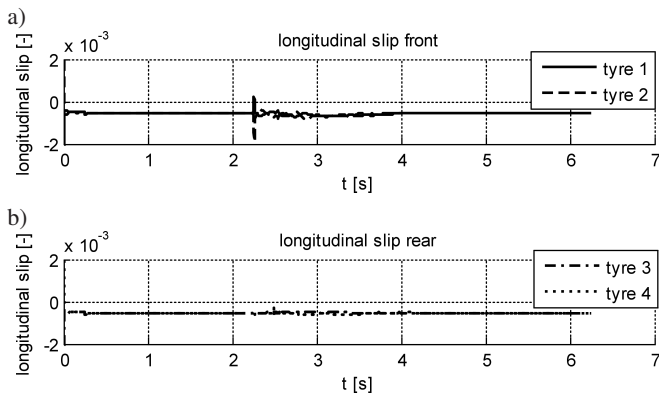
a)

b)

Fig. 13. Waveforms of longitudinal slips of: vehicle wheel tyres: a) front, b) rear

It is convenient to discuss the simulation results individually for each piece of the track. At the initial straight section, the vehicle rolls have no contact with track edges (no contact forces from rollers work on the vehicle). A vehicle moves freely due to the expected clearances of the roller-rail systems. Nevertheless, the vehicle does not move strictly along the ideal centre of the track. The initial sections of the graphs in Fig. 10a describe a minimal increase of the vehicle lateral deviation. It should be noted that on the longer road section the vehicle will reach the state of "sticking" to the rail edge.

At the moment of entry into the turn, the LPZ roller has contact with the rail edge as the first. It causes a short impulse of contact force resulting in a rotation of the vehicle chassis body, however without visible turning of the front and rear wheels (in this time the values of graphs in Fig. 9b are similar). Turning of the front and rear wheels occurs with a certain time delay (when the charts in Fig. 9b continue "spreading out"). A moment of entering the turn is followed by entering into the first transition curve (clothoid), then followed by an exit of the turn along the other transition curve. It is followed by a systematic increase and then by a drop of LPZ roller contact strength. Oscillations are seen of the steering angles of vehicle wheel axle relative to the respective normal to the curvature of the track centre. There is a visible tendency to set a vehicle in the curvature arc shown earlier in Fig. 8. In this setting, the vehicle axle is twisted relative to the movement direction, and LPZ and LT1 rollers provide a contact with the rail edge. The values of angles of twist of the vehicle wheel axle, relative to the normal to the movement curvature, are very important from the point of view of the expected wear of the wheel tread. Figure 10b and 11a show a mutual correlation the discussed values of torsion angles of the front axle and slip angles of front wheels, Fig. 10b and 11a – of steering angles of the rear axle and slip angles of rear wheels. It is worth noting that the maximum value for the required steering angle of wheel axles of the defined turn (at point K – Fig. 3) is $2\alpha_a = 8.10°$. A vehicle without front and rear steering axles could reach such a value of the maximum slip angle. The resultant value for the maximum slip angle of front wheels (in Fig. 12a approx. $3.75°$) is less than this value.

The final part of the movement is the exit from the bend on the straight section. In this fragment of movement, the vehicle moves away from the left edge of the rail. Lack of a centering mechanism does not allow restoration of the vehicle to the coaxial position.

The results obtained from the simulation show that the PRT vehicle dynamics is qualitatively different from the dynamics of a rail vehicle or a car. PRT dynamics differs from the rail vehicle dynamics due to the independence of wheels, no profiling of wheels, no centering mechanism and driving through a system of rollers. PRT vehicle dynamics varies from the car dynamics in a way of entering a bend – a PRT vehicle is nevertheless a rail vehicle, while a car is a man-guided vehicle.

8. The comparative analysis of simulation results

The simulation results are characterized conveniently with the maximum or average values of the slip angle during cornering. The values of the above features for the waveform shown in Fig. 12 are: $\alpha_{1\_max} = 3.7032°$, $\alpha_{1\_max} = 2.3367°$. Figure 13 shows a graph with values of the above features characterising the simulation results taken with differently assumed values of the torsional elasticity c_{r2} of the vehicle wheel axle (The calculations shown in para 8 are made by taking $c_{r2} = 15$ N/rad – see Table 3).
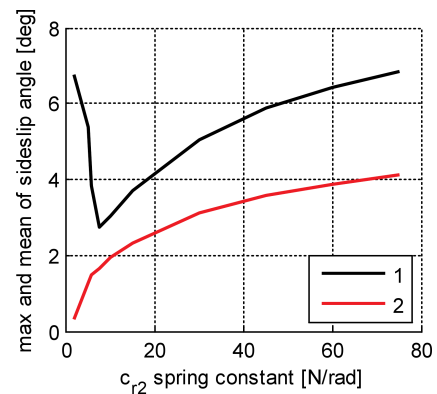

Fig. 14. Graphs of the maximum value (1) and of the slip angle average (2) as a torsional elasticity function of the front axles

The minimum value of the maximum slip angle is achieved by assuming $c_{r2} = 7.5$ N/rad. This is also a limiting value for the range of elasticity values under which you can count on overcoming a bend with stability. For values less than the specified value, the model becomes unstable. One of the reasons for this state is that there are rolling resistance forces of the rollers. For the value $c_{r2} = 5$ N/rad, the simulation results are shown in Figs. 15, 16 and 17.

Figure 15 presents positions of the vehicle axle relative to the track centre: a) lateral deviation, b) steering angles relative to the normal.

Figure 16 shows instantaneous waveforms of forces in the systems of rollers: a) front, b) rear.

Figure 17 represents waveforms of slip angles (sideslip angle alpha) of vehicle wheel tyres: a) front, b) rear.
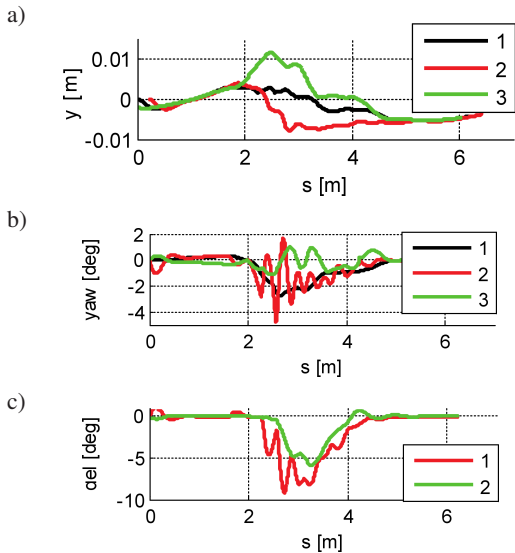
a)

b)

c)

Fig. 15. Graphs of positions of the vehicle axle relative to the track centre in the model with parameter $c_{r2} = 5$ N/rad: a) lateral deviation, b) steering angles relative to the normal. Graphs are marked: 1 $- y_0$, 2 $- y_1$, 3 $- y_2$, 1 $- \psi_0$, 2 $- \psi_1$, 3 $- \psi_2$
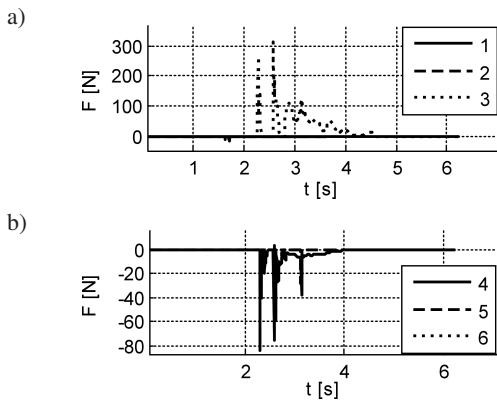
a)

b)

Fig. 16. Instantaneous waveforms of forces in assemblies of rollers in a model with the parameter $c_{r2} = 5$ N/rad: a) front, b) rear. Charts are marked: 1 – LP1, 2 – LP2, 3 – LPZ, 4 – LT1, 5 – LT2, 6 – LTZ
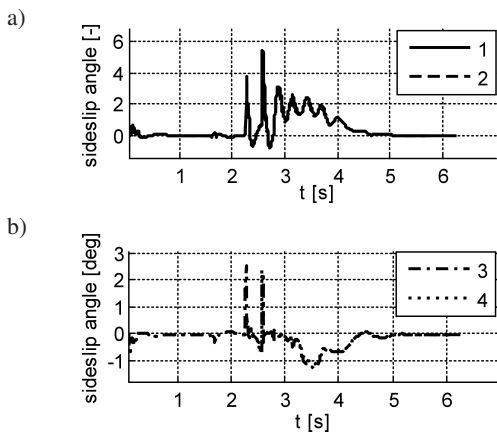
a)

b)

Fig. 17. Waveforms of slip angles (sideslip alpha) of vehicle wheel tyres in a model with the parameter $c_{r2} = 5$ N/rad: a) front, b) rear. Graphs are marked: 1 – left front, 2 – right front, 3 – left rear, 4 – right rear

The results obtained show the presence of significant torsional vibrations to the vehicle model elements when overcoming the bend. Of particular note is the oscillatory nature of instantaneous waveforms of the front axle steering angle, contact forces of rollers and slip angle of the tyres.

9. Final remarks

The results presented show the direction of the required design modifications. No doubt, attention should be paid to the parameters of driving vehicle on the track (guiding rollers, parameters for their contact with the track) in order to reduce vibrations and slipping when driving on the curved track. Driving with the proposed design is different from the classic vehicle, in which the driving is characterised through the contact phenomena of the profiled steel rail-wheel with the profiled rail. It should be emphasized that the phenomena generated by the simulation model corresponds to the qualitative analysis phenomena observed in the physical scale model.

REFERENCES

[1] "Personal rapid transit", http://en.wikipedia.org/wiki/ Personal_rapid_transit.
[2] J.E. Anderson, "A review of the state of the art of personal rapid transit", *J. Advanced Transportation* 343, 29 (2000), DOI: 10.1002/atr.5670340103.
[3] R. MacDonald, "The future of high capacity PRT", *Proc. Thirteenth Int. Conf. Automated People Movers and Transit Systems* 1, CD-ROM (2011).
[4] J. Gustafsson, J. Kang, J. Englund, and P. Grimtell, "Design considerations for capacity in PRT networks", *Automated People Movers and Transit Systems* 2011, 385–394 (2011), DOI: 10.1061/41193(424)35.
[5] R. Swenson, "Solar skyways: mobility in a world beyond oil", *Podcar. City Conf.* 1, 250–262 (2011), DOI: 10.1061/41193(424)24.
[6] M. Kozłowski and W. Choromański, "Dynamics simulation studies on the electric city car with an electromechanical differential and the rear wheels drive", *Bull. Pol. Ac.: Tech.* 61 (3), 661–674 (2013).
[7] W. Choromanski, M. Kozłowski, and I. Grabarek, "Driver – ECO-car system: design and computer simulation of dynamics", *J. Vibroengineering* 17, 411–420 (2015).
[8] S. Iwnicki, *Handbook of Railway Vehicle Dynamic*, Taylor & Francis Group, London, 2006.
[9] W. Choromanski, I. Grabarek, J. Kowara, and B. Kaminski, "Personal rapid transit – computer simulation results and general design principles", *Automated People Movers and Transit Systems* 1, 276–295 (2013).
[10] M. Kozłowski and W. Choromański, "PRT simulation research", *Archives of Transport*. 27–28, 95–102 (2013).
[11] M. Kozłowski, W. Choromański, and J. Kowara, "Parametric sensitivity analysis of ATN-PRT vehicle (Automated Transit Network – Personal Rapid Transit)", *J. Vibroengineering* 17, 1436–1451 (2015).